

Nanoscale

Accepted Manuscript



This is an *Accepted Manuscript*, which has been through the Royal Society of Chemistry peer review process and has been accepted for publication.

Accepted Manuscripts are published online shortly after acceptance, before technical editing, formatting and proof reading. Using this free service, authors can make their results available to the community, in citable form, before we publish the edited article. We will replace this *Accepted Manuscript* with the edited and formatted *Advance Article* as soon as it is available.

You can find more information about *Accepted Manuscripts* in the [Information for Authors](#).

Please note that technical editing may introduce minor changes to the text and/or graphics, which may alter content. The journal's standard [Terms & Conditions](#) and the [Ethical guidelines](#) still apply. In no event shall the Royal Society of Chemistry be held responsible for any errors or omissions in this *Accepted Manuscript* or any consequences arising from the use of any information it contains.



Journal Name

COMMUNICATION

Highly dispersible disk-like graphene nanoflakes.

Vasilios Georgakilas,^{*a} Katerina Vrettos,^a Katerina Katomeri,^a Antonios Kouloumpis,^b Konstantinos Dimos,^b Dimitris Gournis^b and Radek Zboril^c

Received 00th January 20xx,
Accepted 00th January 20xx

DOI: 10.1039/x0xx00000x

www.rsc.org/

We present the preparation of disk-like graphene nanoflakes, highly dispersible in dimethylformamide (DMF), with uniform size and thickness. The preparation procedure includes an overnight mild sonication of natural graphite in DMF, followed by a purification step using ultracentrifugation. The mean diameter of the as produced well round shaped graphene nanoflakes is about 100 nm and they consisted of less than 20 nm graphene monolayers.

In 2004 Novoselov and Geim achieved to isolate single graphene monolayers by a simple micromechanical technique from graphite.¹ The characterisation and the study of physical, chemical, mechanical, electrical and optical properties of this new carbon nanostructure opened new horizons in nanoscience and nanotechnology applications.²⁻⁷ Micromechanical isolation was not capable to produce quantities of graphene for experimental purposes, thus various methods have been developed that produce a plethora of graphene based nanostructures such as pristine graphene⁸⁻¹⁶, graphene oxide (GO)¹⁷⁻¹⁹, partly reduced graphene oxide (rGO)²⁰⁻²⁴, few layers graphene nanosheets, graphene nanoribbons²⁵ or graphene quantum dots (GQD)²⁶⁻²⁹ etc. All these graphene based nanostructures appear remarkable differences in morphology such as the number of layers, graphenic character, size or basic properties such as electrical conductivity, mechanical strength and chemical reactivity.³⁰ The reduction of GO – a product of the strong oxidation of graphite – produces in relatively acceptable yields rGO; a graphenic nanostructure with significant number of remaining oxygen groups and defects that decrease its aromatic character and related properties such as electrical conductivity or mechanical strength.^{17-24,31} On the other hand, pristine

graphene can be isolated directly from graphite by a simple and effective procedure that has been proposed by Coleman et al in 2008⁸ and is based on the ultrasonication of graphite in solvents with surface energy similar to that of graphene. Later, Bourlinos et al showed improved dispersibility of graphene in perfluorinated aromatic solvents and pyridine¹⁰ and other groups in *o*-dichlorobenzene¹¹ and benzylamine¹², DMF^{13,14} using similar procedures. Recently, remarkably longer sonication treatments of graphite, 150 hours in DMF¹⁴ or 460 hours in NMP¹⁵ showed enhanced yields and dispersibilities near 1 mg/mL. It is rather obvious that sonication is one of the most promising techniques to produce not expensive and in good quality graphene nanomaterials³². Following these steps, we present here a simple procedure for the preparation of disk like graphene nanoflakes as a new product of an overnight sonication of graphite in DMF. Disk like graphene nanoflakes have a diameter in the range of 80 – 300 nm and a thickness of 6 nm, indicating that they consisted by 18 - 20 graphenic layers. According to recent literature it could be ideally used in Li ion batteries and other electronic devices as thermal conductors to improve heat removal in combination with materials that can store heat like phase change materials, paraffin waxes etc.³³⁻³⁵ This kind of graphenic nanostructures resemble very much GQDs especially regarding shape and properties and not considering their much larger size. GQDs are usually appeared as products of cutting processes of large graphene nanosheets with a diameter that range between 1 and 20 nm and characteristic photoluminescence properties.²⁶⁻³⁰ The motivation of this procedure was to cover the gap between few hours sonication methods that produce diluted dispersion of single layer graphene mixed with few layer graphene and extremely long sonication procedures of 150 or 460 hours that produce similar products with increased dispersibility, in liquid exfoliation of graphite.^{14,15} The present procedure includes an overnight sonication of natural graphite in DMF, combined with a purification-isolation step of ultracentrifugation. The product of this work could be seen as a novel graphenic material that has not been appeared up to now in the literature. In fact, unique disk-like graphene

^a Department of Materials Science, University of Patras, 26504 Rio (Greece)

^b Department of Materials Science and Engineering, University of Ioannina, 45110 Ioannina (Greece)

^c Regional Centre of Advanced Technologies and Materials, Faculty of Science, Department of Physical Chemistry, Palacky University in Olomouc, Olomouc 77146 (Czech Republic).

† Footnotes relating to the title and/or authors should appear here. Electronic Supplementary Information (ESI) available: [details of any supplementary information available should be included here]. See DOI: 10.1039/x0xx00000x

nanoflakes with 6 nm thickness, 100 nm mean diameter and well defined round shaped are the main product of this procedure. Up to now, only large graphene sheets with random shape have been produced by a variety of exfoliation methods using graphite as precursor⁹ or extremely small graphene quantum dots using other methods.²⁶⁻³⁰ The most relevant GQDs to the present graphene nanoflakes, with mean diameter near 60 nm, a thickness of 2-3 nm and well defined round shape have been produced by Mullen et al using a bottom up approach that based on the pyrolysis of self assembled hexa-peri-hexabenzocoronene nanostructures.³⁶

The size of the disk-like graphene nanoflakes is crucially large, maintaining important properties such as electrical conductivity and on the other hand, is small enough and even ideal in some cases, for application in bionanotechnology, nanomedicine and drug delivery, micromanipulation, nanochemistry etc. It is furthermore very important that graphene nanoflakes remain dispersible in DMF even after centrifugation at 13000 rpm. A schematic representation of the procedure is presented in Fig. 1. Briefly, the starting carbon material - natural graphite - suspended in DMF was sonicated continuously overnight and the supernatant was isolated from the precipitate after three days standing.

As presented in Figure 2 the main product of the overnight sonication of graphite was round shaped in the majority few layer graphene nanoflakes with a diameter that range between 50 and 500 nm. The larger graphene nanoflakes were often covered by carbon nanoparticles. According to blank experiments, the origin of these unwanted carbon nanoparticles was organic contaminants of the solvent that probably were organised to amorphous carbon nanoparticles due to the sonication procedure. The reproducibility of the procedure has been examined and furthermore it was also concluded that further sonication up to 48 hour had no remarkable impact in the morphology of the product but improved the yield leading to more concentrated dispersions (see Figure 2b).

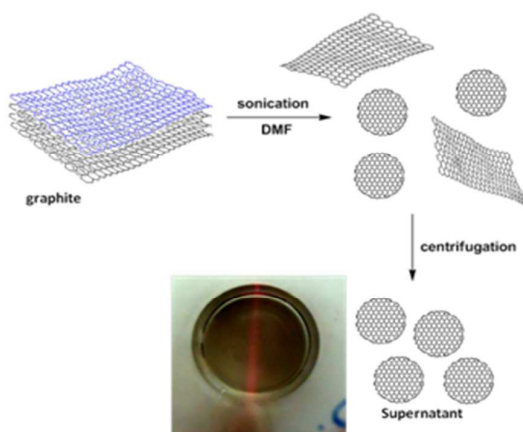


Fig. 1. Schematic representation of the preparation of graphene nanoflakes. The inserted photo the Tyndall effect verifies the presence of colloidal nanostructures in the DMF solution.

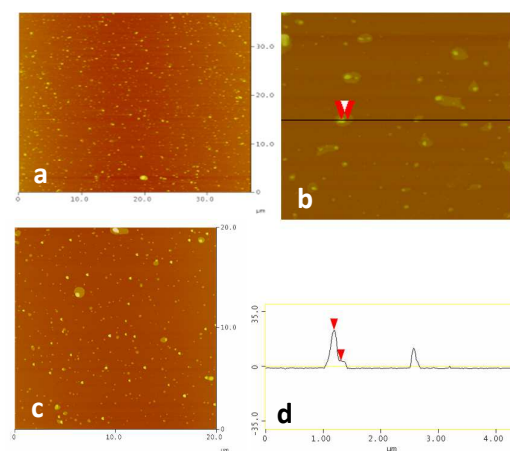


Fig. 2. AFM images of highly dispersed graphene nanoflakes (a,b) after 24 hours and (c) after 48 hours sonication before purification step. (d) section analysis on image b.

For the isolation of disk like graphene nanoflakes, an ultracentrifugation step followed where large graphene nanosheets covered by carbon nanoparticles were removed from the liquid phase by precipitation leaving a light grey diluted supernatant that was isolated and remained stable over several months (see Figure 3b). As presented in Figure 3, the highly dispersible graphene nanoflakes was the main product after the purification step and appeared free of carbon nanoparticle impurities and large graphene flake by-products (see also Electronic Supplementary Information (ESI)).

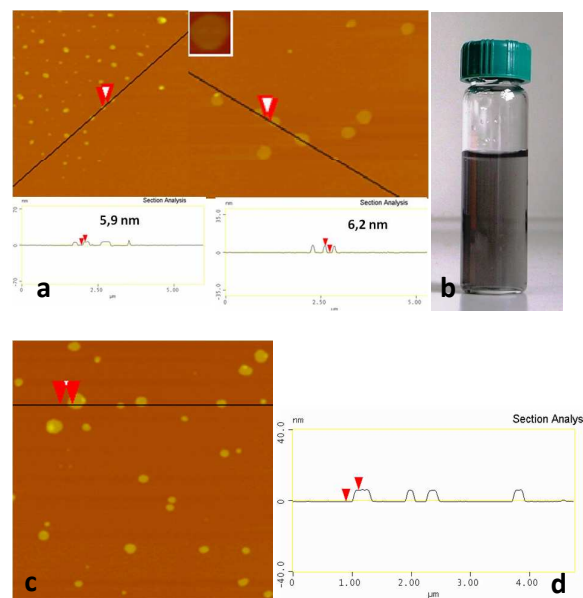


Fig. 3. (a) AFM and section analysis of highly dispersible purified graphene nanoflakes and (b) photo of the dispersion of disk like graphene nanoflakes in DMF. (c) AFM image of the product after 48 hours sonication and ultracentrifugation and (d) section analysis of the finally isolated disk like graphene nanoflakes.

Graphene nanoflakes were stable in DMF (~0.05 mg/mL) without precipitation for several months. A careful estimation of the size distribution showed that the majority of graphene nanoflakes (70-80%) have a diameter between 80 and 120 nm, while a lower percentage (about 15%) have a diameter between 60 and 80 nm and the rest between 200 and 300 nm. As regards the number of the layers, the great majority (over 90 %) of graphene nanoflakes have a thickness around 6 nm which indicates a number of layers between 18 and 20.

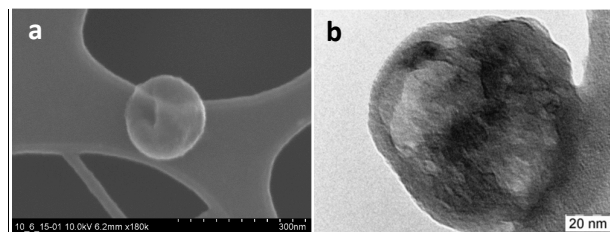


Fig 4. a) SEM and b) High-resolution TEM images of disk-like graphene nanoflakes.

Figure 4a presents a SEM image of a characteristic disk-like graphene nanoflake (see also ESI). A characteristic HRTEM image of the disk like graphene nanoflake is also shown in figure 4b, whereas various crystal planes are observed along with hollow-like (lower contrast) parts indicating that the disks are composed of overlapped ultrathin nanoflakes creating unique rounded morphology. In general similar round shape disk like nanoflakes with less mean diameter are presented in the supernatant after centrifugation at 15000 rpm, whereas at 8000 rpm several larger graphene nanosheets were also presented in the supernatant (see ESI) showing that the speed of the centrifugation has an impact in the mean size and the morphology of the isolated graphene nanostructures.

The Raman spectrum of these nanoflakes showed the characteristic D (1350 cm^{-1}) and G (1582 cm^{-1}) bands and an I_D/I_G ratio of 0.21 that is mainly attributed to the high percentage of carbon atoms that are placed in the circumference of the flakes (rich in sp^3 carbon atoms) due to their small size. The low I_D/I_G ratio combined with the small size indicates a highly aromatic character for these nanoflakes. This is further verified by the characteristic single and sharp 2D band at 2700 cm^{-1} and the high I_{2D}/I_G ratio of 1.02 which are in accordance with the few number of graphene layers that appeared in the product (see Fig. 5).³⁷ In the same figure, the Raman spectrum of the unpurified product is also presented. A much lower I_D/I_G ratio of 0.11 here reflects the contribution of larger graphene nanoflakes that are present in the unpurified product. In addition, I_{2D}/I_G ratio is nearly twice for the purified product compared to I_{2D}/I_G of the crude product, whereas the 2D band is asymmetric exhibiting a maximum at 2720 cm^{-1} . Thus, the enhanced intensity and a significant shift of the 2D peak of the sample after centrifugation clearly suggest the successful purification of the product. The XPS analysis of the unpurified product – before centrifugation- showed that the dispersed graphitic material was enriched with oxygen groups.

More specifically from the C1s photoelectron peak various different chemical groups of carbon were received.

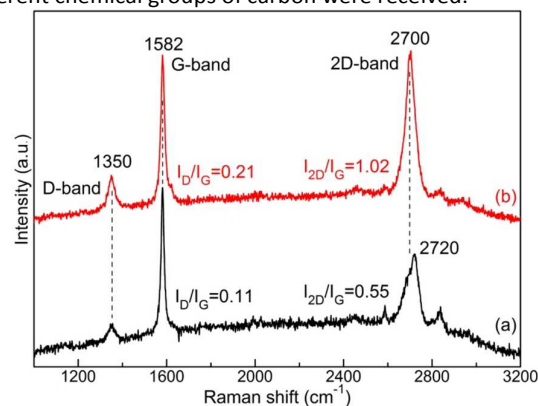


Fig. 5. Raman spectra of the as produced (a) and the purified (b) graphene nanoflakes.

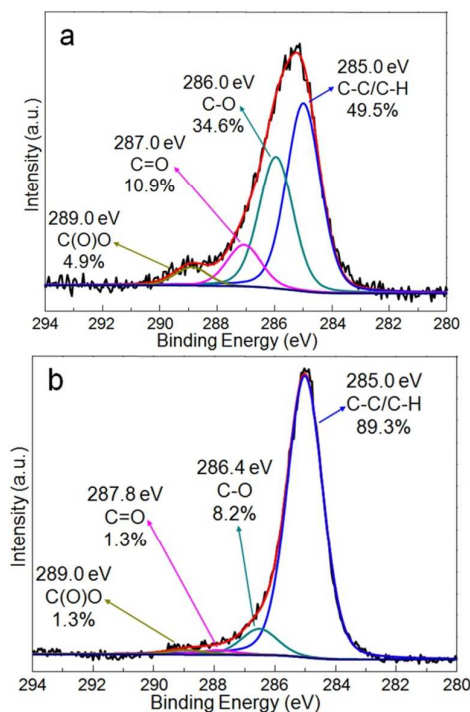


Fig. 6. a) The XPS analysis of the dispersed graphitic nanostructures before centrifugation. b) The XPS analysis of the purified graphene nanoflakes.

The C-C peak at 285.0 eV was assigned to the hexagonal lattice of graphene (C-C bonds) and contributed 49.5% of the whole carbon area. The C-O and C-OH groups (286.0 eV) decorated probably on the surface of the graphene sheets consisted of 34.6% of the total carbon amount. Furthermore the creation of carbonyl and carboxyl groups centered at 287.0 eV and 289.0 eV of the photoelectron peaks and accounted 10.9 % and 4.9 % of the total carbon intensity respectively was recorded (see Fig. 6).

Interestingly, the XPS analysis of the purified nanographenes, after the centrifugation at 13000 rpm, showed limited appearance of oxygen groups. In fact, the percentage of C-C bonds (peak at 285.0 eV) was very high reaching 89.3%, while C-O functional groups (peak at 286.4 eV) were limited to 8.2% of the carbon intensity and carbonyl and carboxyl groups were slightly over 1% of the carbon peak respectively. The results of the XPS analysis are in accordance with Raman spectroscopic data as regards the high graphitic character of graphene nanoflakes and indicate the determining role of ultracentrifugation in the removal of the unwanted carbon nanoparticles. The characteristic difference as regards the presence of defects seems to be the key factor in the transformation of the -enriched in defects- large graphene nanosheets to the final defect free disk like nanoflakes. Figure 7 presents a characteristic part of the sonication product where a large graphene nanoflake is cut in smaller pieces and finally in small graphene disk-like nanoflakes.

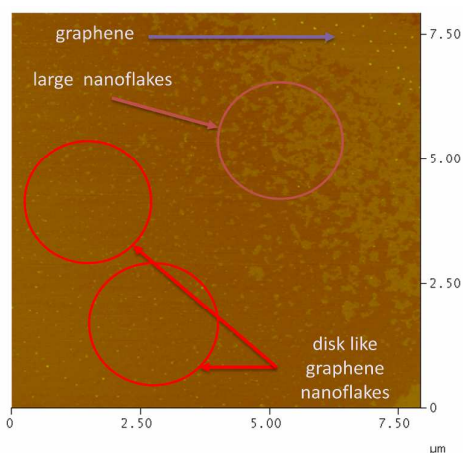


Figure 7. AFM image of the graphenic products after 24 hours sonication. The graphene nanosheets are cut in smaller pieces and finally in small disk like graphene nanoflakes.

The UV-Vis spectrum of graphene nanoflakes suspended in DMF has a main peak at 272 nm due to $\pi-\pi^*$ of C=C bonds which is continuously decreasing from 272 nm to 600 nm. The unpurified product -before centrifugation- showed lower absorption with a maximum slightly shifted at 270 nm, while the curve starts at higher values due to the scattering of the light on the large graphene aggregates. On the other hand, the UV-Vis spectrum of the finally isolated graphene nanoflakes showed higher absorption and much lower scattering verifying the relatively small size of the dispersed graphene nanostructures (see Fig 8, upper). Photoluminescence characterization indicated that graphene nanoflakes emit violet to blue PL under excitation at 320 to 380 nm (fig 8, down). Three dominant, excitation-independent states are observed for the PL emission at 390, 410, and 435 nm while a shoulder is nearly detected in all four spectra at 470 nm. Changing the excitation wavelength from 320 to 380 nm, the main PL peak possesses decreased intensity and is shifted from 390 to 435 nm. The most intense PL emission appears under

340 nm excitation and has a maximum at 410 nm. The same energy release pathway, i.e. at 410 nm, is followed when excitation at 360 nm occurs, whilst in all cases PL from the rest states is also observed. The unpurified product where the major part is large graphene nanoflakes and nanosheets, exhibits very low, almost no detectable, PL emission.

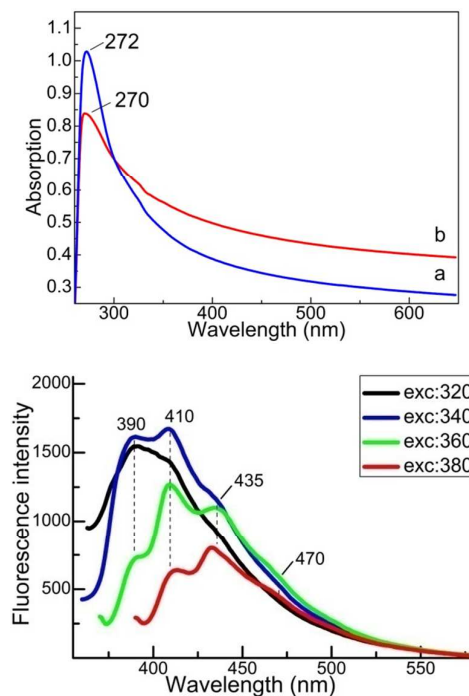


Fig. 8. (upper) UV-Vis spectra of graphene nanoflakes a) after centrifugation, and b) before centrifugation. (down) PL spectra of graphene nanoflakes at several excitation wavelengths.

The PL properties of graphene nanoflakes could be complementary to that of GQDs since the nanoflakes demonstrate violet to blue PL whereas GQDs emit blue light in most cases. The quantum yield (QY) is significantly high -about 10%- regarding the mean size of the nanoflakes and the QY of the much smaller GQDs and is reasonable due to the percentage of PL active smaller graphene nanoflakes in the final product.³⁸ Further research in this subject is in progress, since the findings of this work showed among else that centrifugation could be used to control the content of the final graphenic product of the liquid exfoliation method and regarding graphene nanoflakes, PL emission could be a powerful tool for their characterisation and estimation of size distribution.

Conclusions

In conclusion, the overnight sonication of graphite in DMF, in combination with a centrifugation step at 13000 rpm produces high quality, almost monodispersed, disk-like graphene nanoflakes with a thickness of 6 nm and a diameter around 100 nm. Importantly the finally isolated nanographenes were highly dispersible and stable in DMF. According to the results of the procedure that is described here, it is expected that

morphological characteristics such as size, shape and thickness of graphene products could be predicted by controlling the conditions of graphite sonication and the purification steps.

Notes and references

‡ **Preparation of graphene nanoflakes.** The graphite powder was supplied by NUKEM GmbH (Germany). 10 g of natural graphite is mixed with 50 mL of DMF and the mixture is sonicated continuously for 24 hours or 48 hours (ultrasonic bath, Branson 2050E-MT, 100 Watt, 40 kHz). After the sonication, the mixture is stand overnight and then the supernatant is centrifuged at 13000 rpm for 15 min. The supernatant was isolated and kept in glass bottle without precipitation after several months.

Measurements and characterization. Raman spectroscopy was performed on a Micro-Raman system RM 1000 RENISHAW using a laser excitation line at 532 nm (Nd-YAG). A power of 0.5-1 mW was used with a 1 μ m focus spot in order to avoid photodecomposition of the samples. AFM images were obtained in tapping mode with a 3D Multimode Nanoscope, using Tap-300G silicon cantilevers with a tip radius <10 nm and a force constant of \approx 20–75 N.m⁻¹. Samples were deposited onto silicon wafers (P/Bor, single side polished) from DMF solutions by drop casting. X-ray photoelectron spectroscopy (XPS) measurements were performed under ultrahigh vacuum conditions with a base pressure of 5×10^{-10} mbar in a SPECS GmbH instrument equipped with a monochromatic MgK α source ($h\nu = 1253.6$ eV) and a Phoibos-100 hemispherical analyser. Samples were dispersed in H₂O (1 wt %), and after short sonication and stirring, a minute quantity of the suspensions was drop cast on silicon wafers and left to dry in air before transfer to ultrahigh vacuum. The energy resolution was set to 0.3 eV and the photoelectron take-off angle was 45° with respect to the surface normal. Recorded spectra were the average of 3 scans with energy step set to 0.05 eV and dwell time 1 sec. All binding energies were referenced to the C1s core level at 285.0 eV. Spectral analysis included a Shirley background subtraction and peak deconvolution employing mixed Gaussian–Lorentzian functions, in a least squares curve-fitting program (WinSpec) developed at the Laboratoire Interdisciplinaire de Spectroscopie Electronique, University of Namur, Belgium. PL spectra were recorded by a Hitachi F-2500 fluorescence spectrometer. The optical spectra were recorded in quartz cuvettes by using a Shimadzu UV2100 spectrophotometer.

Acknowledgements.

The authors thank P. Bazgerová and O. Tomanec for Radka Kralova for AAS analysis, Dr. V. Ranc for GC analysis and Dr. J. Tucek for technical assistance. The authors acknowledge support from the Ministry of Education, Youth and Sports of the Czech Republic (LO1305).

References

- 1 K.S. Novoselov, A.K. Geim, S.V. Morozov, D. Jiang, Y. Zhang, S.V. Dubonos et al. *Science*, 2004, **306**, 666.
- 2 A.K Geim, K.S Novoselov, *Nature Materials*, 2007, **6**, 183.
- 3 A.K Geim, *Science*, 2009, **324**, 1530.
- 4 D.R. Dreyer, R.S. Ruoff, C.W. Bielawski, *Angewandte Chemie Int. Ed.*, 2010, **49**, 9336.
- 5 P. Avouris, *Nano Letters*. 2010, **10**, 4285.
- 6 X. Huang et al. *Small* 2011, **7**, 1876.
- 7 V.I. Fal'ko, L. Colombo, P.R. Gellert, M.G. Schwab, K. Kim, K.S. Novoselov, *Nature*, 2012, **490**, 192.
- 8 Y. Hernandez, V. Nicolosi, M. Lotya, F.M. Blighe, Z.Y. Sun, S. De, I.T. McGovern, B. Holland, M. Byrne, Y.K. Gun'ko, J.J. Boland, P. Niraj, G. Duesberg, S. Krishnamurthy, R. Goodhue,

- J. Hutchison, V. Scardaci, A.C. Ferrari, J.N. Coleman, *Nat. Nanotechnol.*, 2008, **3**, 563.
- 9 M. Cai, D. Thorpe, D.H. Adamson, H.C. Schniepp, *J. Mater. Chem.*, 2012, **22**, 24992.
- 10 A.B. Bourlinos, V. Georgakilas, R. Zboril, T.A. Steriotis, A.K. Stubos, *Small*, 2009, **5**, 1841.
- 11 C.E. Hamilton, J.R. Lomeda, Z. Sun, J.M. Tour, A.R. Barron, *Nano Lett.*, 2009, **9**, 3460.
- 12 S.P. Economopoulos, G. Rotas, Y. Miyata, H. Shinohara, N. Tagmatarchis, *ACS Nano*, 2010; **4**: 7499–7507.
- 13 V. Georgakilas, A. Kouloumpis, D. Gournis, A. Bourlinos, C. Trapalis, R. Zboril, *Chemistry - A European Journal*, 2013, **19**, 12884.
- 14 U. Khan, P. May, A. O'Neill, J.N. Coleman, *Carbon*, 2010; **48**: 4035.
- 15 U. Khan, A. O'Neill, M. Lotya, S. De, J.N. Coleman, *Small*, 2010, **6**, 864.
- 16 K. Parvez, Z.S. Wu, R. Li, X. Liu, R. Graf, X. Feng, K. Müllen, *J. Am. Chem. Soc.*, 2014, **136**, 6083.
- 17 O.C. Compton, S.T. Nguyen, *Small*, 2010, **6**, 711.
- 18 Y. Zhu, S. Murali, W. Cai, X. Li, J.W. Suk, J.R. Potts, R.S. Ruoff, *Advanced Materials*, 2010, **22**, 3906.
- 19 J.I. Paredes, S. Villar-Rodil, A. Martínez-Alonso, J.M.D. Tascón, *Langmuir*, 2008, **24**, 10560.
- 20 S. Park, J.H. An, I.W. Jung, R.D. Piner, S.J. An, X.S. Li, A. Velamakanni, R.S. Ruoff, *Nano Lett.* 2009, **9**, 1593.
- 21 S. Stankovich, D.A. Dikin, R.D. Piner, K.A. Kohlhaas, A. Kleinhammes, Y. Jia, Y. Wu, S.T. Nguyen, R.S. Ruoff, *Carbon* 2007, **45**, 1558.
- 22 C.K. Chua, M. Pumera, *Chem. Soc. Rev.*, 2014, **43**, 291.
- 23 T. Kuila, A.K. Mishra, P. Khanra, N.H. Kim, J.H. Lee, *Nanoscale*, 2013, **5**, 52-71.
- 24 S. Pei, H.M. Cheng, *Carbon*, 2012, **50**, 3210.
- 25 M. Terrones, A.R. Botello-Méndez, J.C. Delgado, F.L. Urías, Y.I.V. Cantú, F.J.R. Macías, A.L. Elías, E.M. Sandoval, A.G. Cano-Márquez, J.C. Charlier, H. Terrones, *Nano Today*, 2010, **5**, 351.
- 26 F. Liu, M.H. Jang, H.D. Ha, J.H. Kim, Y.H. Cho, T.S. Seo, *Advanced Materials*, 2013, **25**, 3657.
- 27 J. Shen, Y. Zhu, C. Chen, X. Yang, C. Li, *Chem. Commun.*, 2011, **47**, 2580.
- 28 M. Bacon, S.J. Bradley, T. Nann, *Part. Part. Syst. Character.* 2013, DOI: 0.1002/ppsc.201300252.
- 29 Q. Xue, H. Huang, L. Wang, Z. Chen, M. Wu, Z. Li, D. Pan, *Nanoscale*, DOI: 10.1039/c3nr03623e.
- 30 V. Georgakilas, J.A. Perman, J. Tucek, R. Zboril, *Chem. Rev.* 2015 (asap).
- 31 D. Li, M.B. Muller, S. Gilje, R.B. Kaner, G.G. Wallace, *Nat. Nanotechnol.* 2007, **3**, 101.
- 32 W. Du, X. Jiang, L. Zhub, *J. Mater. Chem. A*, 2013, **1**, 10592.
- 33 P. Goli, S. Legedza, A. Dhar, R. Salgado, J. Renteria, A.A. Balandin, *Journal of Power Sources* 2014, **248**, 37.
- 34 A.A. Balandin, *Nature Materials* 2011, **10**, 569.
- 35 K.M.F. Shahil, A.A. Balandin, *Nano Lett.* 2012, **12**, 861.
- 36 R. Liu, D. Wu, X. Feng, K. Mullen, *J. Am. Chem. Soc.* 2011, **133**, 15221.
- 37 A.C. Ferrari, J.C. Meyer, V. Scardaci, C. Casiraghi, M. Lazzeri, F. Mauri, S. Piscanec, D. Jiang, K.S. Novoselov, S. Roth, A.K. Geim, *Phys. Rev. Lett.* 2006, **97**, 187401.
- 38 S. Zhu, J. Zhang, X. Liu, B. Li, X. Wang, S. Tang, Q. Meng, Y. Li, C. Shi, R. Hu, B. Yang *RSC Advances*, 2012, **2**, 2717–2720.